

María J. Taulamet, Néstor J. Mariani, Guillermo F. Barreto and Osvaldo M. Martínez*

A critical review on heat transfer in trickle bed reactors

Abstract: A critical review of the available information about heat transfer between a packed bed with cocurrent downflow of gas and liquid and an external medium was undertaken. Several aspects such as experimental set-ups and methods employed to study heat transfer in trickle bed reactors, models used to interpret experimental data, and literature correlations of heat transfer parameters are addressed. From the analysis of the available experimental information, a refined database has been built, which allows comparing the performance of the existing correlations for the parameters of the extensively employed two-dimensional pseudohomogeneous plug flow model (i.e., effective radial thermal conductivity and wall heat transfer coefficient). In addition, new correlations for effective thermal conductivity have been developed. Identification of gaps in the current knowledge and recommendations for future works are summarized.

Keywords: heat transfer mechanisms; heat transfer models; radial thermal conductivity; trickle bed reactors; wall heat transfer coefficient.

DOI 10.1515/revce-2014-0050

Received October 21, 2014; accepted December 31, 2014; previously published online March 18, 2015

1 Introduction

Catalytic gas-liquid reactors, in particular fixed bed reactors with cocurrent downflow, widely known as trickle bed reactors (TBR), have been commonly employed in

petroleum refining and petrochemistry. Hydrotreating processes, such as hydrodesulfurization, hydrorefining, hydrodenitration, and hydrocracking (Martínez et al. 1994, Ancheyta 2011); hydrogenation reactions (Bressa et al. 1998); and hydrocarbon synthesis by the Fischer-Tropsch process (Krishna and Sie 1999, Zhu 2013) are frequently carried out in TBR. In addition, out of the above traditional applications, the use of TBR has been extended into new fields such as biochemical, electrochemical, and waste-treatment processes, including oxidation of harmful organic compounds (Levec and Pintar 1995, Ranade et al. 2011).

The conceptual and practical aspects of TBR have been intensively studied over the last four decades, and several relevant reviews on the subject can be found in the literature: Zhukova et al. (1990), Gianetto and Specchia (1992), Saroha and Nigam (1996), Al-Dahhan et al. (1997), Dudukovic et al. (1999), and Mederos et al. (2009). These articles provide general information about the models and parameters employed to represent the behavior of TBR, but they do not deal in depth with every particular aspect. Among the many issues involved in modeling TBR, heat transfer phenomenon is of special importance, and it will be the focus of the present review.

In general terms, to study transport processes, particularly heat transfer in fixed beds, two levels can be defined: bed scale and particle scale.

At the particle scale, heat transfer can be adequately described using a solid-fluid heat transfer coefficient (Mancandelli et al. 1999, Boelhouwer et al. 2001, Bandari et al. 2012, Heidari and Hashemabadi 2013). In the case of TBR, it is usual to assume that particles are surrounded by a liquid film; nonetheless, this hypothesis should be revised for low liquid superficial velocities due to the nonuniform wetting of the particle surface (Ranade et al. 2011).

To analyze the bed level, two alternatives should be considered: adiabatic or cooling/heating operation. Several processes, such as methyl-isobutyl ketone synthesis or Fischer-Tropsch process, require exchanging heat with an external medium using a multitubular reactor, and specifically in the last case, heat transfer is highly improved by the presence of the liquid phase (Jess and Kern 2012). Thus, the heat transfer processes become determining of the global reactor behavior. Heat transfer

*Corresponding author: Osvaldo M. Martínez, Facultad de Ingeniería, PROIRQ, Departamento de Ingeniería Química, UNLP, La Plata, Argentina, e-mail: ommartin@ing.unlp.edu.ar; and Centro de Investigación y Desarrollo en Ciencias Aplicadas “Dr. J. J. Ronco” (CINDECA), CCT La Plata-CONICET-UNLP, calle 47 No. 257, CP B1900AJK, La Plata, Argentina

María J. Taulamet, Néstor J. Mariani and Guillermo F. Barreto: PROIRQ, Facultad de Ingeniería, Departamento de Ingeniería Química, UNLP, La Plata, Argentina; and Centro de Investigación y Desarrollo en Ciencias Aplicadas “Dr. J. J. Ronco” (CINDECA), CCT La Plata-CONICET-UNLP, calle 47 No. 257, CP B1900AJK, La Plata, Argentina

also plays an important role in laboratory and bench-scale TBR devoted to study catalyst behavior due to the fact that an isothermal operation is highly convenient for the purpose of data analysis (Mary et al. 2009, Mederos et al. 2009).

For adiabatic reactors, especially industrial units, knowledge of heat transport capacity inside the bed, usually quantified through an effective thermal conductivity, is of paramount importance. Local hot spots can arise when exothermic reactions are carried out (Ranade et al. 2011, Mousazadeh 2013), owing to an insufficient capacity to disperse heat.

In this context, a critical review of the open literature about heat transfer at the bed scale is proposed with two objectives: on the one side, to gather a set of correlations of heat transfer parameters that can be considered as the most consistent one, and on the other side, to identify operative and geometric conditions for industrial and laboratory units for which experimental information is scarce and also the correlations cannot be used confidently.

Finally, considering that one of the most common alternatives to TBR is the use of packed beds with cocurrent up-flow, some comments about heat transfer in the latter system are also included.

The following issues are addressed in this review:

- experimental set-ups and methods employed to study heat transfer in TBR;
- models used to interpret experimental data;
- analysis and discussion of the available experimental data and correlations of heat transfer parameters;
- heat transfer in packed beds with cocurrent up-flow; and
- recommendation of correlations and identification of gaps in the current knowledge.

In the development of this review, it will become apparent that there are two crucial aspects whose prior knowledge is essential for a correct evaluation of heat transfer in TBR: bed packing features and fluid-dynamic characterization of the system. According to the scope of this contribution, these aspects will not be systematically discussed, but due consideration about them will be provided, as required.

2 Experimental set-ups and methods

Different alternatives for the experimental set-up can be employed whether the heat transfer study is focused on

particle or bed level. In this review, the interest is oriented toward the last aspect.

The most extensively used experimental set-up involves the analysis of heat transfer through the cylindrical wall of a packed tube, inside which the two fluid phases flow cocurrently downward. This traditional set-up was employed in several works (Weekman and Myers 1965, Hashimoto et al. 1976, Muroyama et al. 1977, Matsuura et al. 1979a,b, Specchia and Baldi 1979, Colli Serrano 1993, Lamine et al. 1996, Babu and Sastry 1999, Mariani 2000, Mariani et al. 2001, Borremans et al. 2003, Pinto Moreira 2004, Babu and Rao 2007, Babu et al. 2007). As a heat source (or sink), an external fluid (with or without phase change) or an electric resistance can be used. The set of temperature measurements also varies. For the incoming fluids, an average or distributed (both radially and angularly) temperature can be recorded. On the contrary, a radial temperature distribution is usually measured at the bed outlet at a single or at several angular positions. Measures at different axial positions can be obtained by introducing sensors, typically thermocouples, inside the bed. Depending upon the number of sensors to be introduced, this assemblage can disturb the flow of fluids. A better alternative was implemented by Mariani (2000), who divided the heating jacket into three sections that can be activated independently. In this way, it was possible to work with different heat exchange heights (by activating one, two, or three sections of the jacket) without introducing sensors at different heights.

The experimental data obtained from this approach allow estimating an overall heat transfer coefficient or, provided that a two-dimensional model is used, values of effective thermal conductivity and wall heat transfer coefficient. For the effect of some aspects, as bed length and the configuration of angular and radial temperature measurements on heat transfer result, it is useful to consult the work of Dixon (2012), taking into account that this kind of experimental set-up has been also typically used in heat transfer studies in packed beds with single-phase flow.

A second type of set-up is intended to evaluate only the effective thermal conductivity. An adiabatic bed is fed with two fluid streams at different temperatures that are conveyed into the bed through two separated zones of the cross-section. The sharp temperature distribution at the top of the bed becomes progressively blurred along the bed, due to the lateral mixing, and analysis of the experimental cross-section profiles allows estimating the effective thermal conductivity. In any case, care should be taken to avoid that the mixing effects reach the bed walls. Crine (1982) employed a cylindrical bed, feeding a hot liquid stream in the cross-section core and a cold

liquid stream in the annulus (the gas flow in each zone is assumed to enter at thermal equilibrium with the liquid). Grosser et al. (1996) used a bed of square-section divided in halves for the hot and cold fluid streams.

For a third type of set-up, as implemented by Mousazadeh et al. (2012), gas and liquid flow in an annular packed bed, where the inner and outer walls are in contact with hot and cold sources at uniform temperatures. Far enough from the bed inlet, a constant heat flux in the radial direction is developed and a stationary temperature profile is generated.

Tables 1 and 2 summarize the main features of experimental set-ups employed to study heat transfer in packed beds with cocurrent two-phase downflow. It can be advanced that the main experimental results were obtained using air and water as fluids in beds of spherical particles. A detailed analysis about these aspects will be performed in Sections 4.1.2 and 4.1.5. The work of Mousazadeh et al. (2012) is not included in Tables 1 and 2 because of the reasons given in Section 3.

3 Models used to interpret experimental data

3.1 Cylindrical packed beds with heat exchange through the walls

When the first experimental set-up mentioned in the Section 2 is selected, the one-dimensional pseudohomogeneous model is the simplest alternative to interpret the experimental data. This model, presenting the global heat transfer coefficient as a single parameter, has been widely used in packed beds with single-phase flow (Lemcoff et al. 1990) but scarcely employed with two-phase flow (Mariani et al. 2001). For TBR, the most extensively used is the two-dimensional pseudohomogeneous plug flow (2DPPF) model. The heat balance equation for this model, relying on the usual hypothesis of steady-state operation, negligible local temperature difference among the phases, axisymmetry, and negligible axial thermal dispersion, reads:

$$(Lc_{PL} + Gc_{PG}^*) \left[\frac{\partial T}{\partial z} \right] = \frac{1}{r} \frac{\partial}{\partial r} \left[k_{er} r \frac{\partial T}{\partial r} \right], \quad (1)$$

where c_{PG}^* is a modified specific heat accounting for the partial vaporization of the liquid phase,

and $c_{PG}^* = \frac{\hat{H}_E - \hat{H}_0}{\bar{T}_E - T_0}$,

where \hat{H}_0 and \hat{H}_E are the enthalpies of saturated air-steam per unit mass of dry air at the bed-inlet and bed-exit mean temperatures (T_0 and \bar{T}_E), respectively.

Regarding axial thermal dispersion, Pinto Moreira et al. (2006) concluded that its inclusion does not improve the quality of fitting of the remaining thermal parameters.

To solve Eq. (1), two boundary conditions in the radial direction and one initial condition are required. Radial symmetry imposes the first boundary condition:

$$\frac{\partial T}{\partial r} = 0 \quad \text{at } r=0. \quad (2a)$$

The simplest alternative for the second boundary condition is

$$T = T_w \quad \text{at } r=R_t. \quad (2b)$$

Eqs. (2a) and (2b), along with a uniform value of k_{er} in Eq. (1), was employed by Weekman and Myers (1965). Later on, Specchia and Baldi (1979) and Pinto Moreira et al. (2006) pointed out that the approach of Weekman and Myers is not adequate to obtain reliable values of k_{er} . Actually, radial thermal conductivity cannot be uniform because bed structure is not uniform. Thus, for regions far from the tube wall, the packing can be considered as random, but in the wall region, particles become more orderly packed because of the effect of the wall (e.g., Mariani et al. 1998). Thus, it is not suitable to assume a uniform value of k_{er} along with condition (2b), unless the ratio between tube and particle diameters is large enough (say, higher than 20–30) to minimize wall effects. The previous considerations indicate that values of k_{er} reported by Weekman and Myers (1965) cannot be considered for further analysis.

One possibility to retain boundary condition (2b) is to assume a variable radial thermal conductivity. To the best of our knowledge, this approach has been employed for single fluid flow in packed beds (Dixon 2012), but not for two-phase flow.

The most widely used boundary condition at the tube wall includes a wall heat transfer coefficient (h_w) accounting for the distinct thermal features close to the wall, while keeping a uniform radial thermal conductivity. Thus,

$$-k_{er} \frac{\partial T}{\partial r} = h_w [T_w - T(R_t)] \quad \text{at } r=R_t. \quad (2c)$$

Eq. (1), boundary conditions (2a) and (2c), and assuming a constant value of T_w and uniform temperature value at the bed inlet,

$$T(r) = \bar{T}_0 \quad \forall r, \quad \text{at } z=0 \quad (2d)$$

Table 1: Geometric features and packings employed in experimental heat transfer studies in TBR.

Authors	Particle shape	Material	d_p (mm)	$a=d_r/d_p$	d_r (mm)	L (m)
Weekman and Myers (1965)	Spheres	TCC Glass Alumina	3.78 4.75 6.48	20.16 16.04 11.76	76.2	0.6096
Hastimoto et al. (1976)	Spheres	Glass Alumina	2.6/4.8 4.4	28.38/15.38 16.77	73.8	1
Specchia and Baldi (1979)	Spheres	Glass Ceramic	6 12.9	23.5 10.93	141	0.35
Matsuura et al. (1979a,b) Crine (1982)	Rings Spheres Spheres	Ceramic Glass γ -Alumina Glass	6 1.2/2.6/4.3 2.2	63.33/29.23/17.67 272.73	76 600	0.6 0.97
Grosser et al. (1996)	Spheres	Urea-formaldehyde	11.1/15.0/25.4	18.92/14/8.27	210×210^b	1.06
Lamine et al. (1996) Babu and Sastry (1999); Babu and Rao (2007); Babu et al. (2007)	Spheres Spheres Spheres Raschig rings	Glass Glass Ceramic Ceramic	5.5/4.5/2.0 2.0/6.0 4.05/6.75 4.0/6.75	38.18/46.67/105 50/16.67 12.35/7.41 10.22/6.17 ^c	100 50 50	1 0.715
Mariani et al. (2001) Borremans et al. (1993)	Spheres	Glass	2.59	19.3		
Colli Serrano (2003) Pinto Moreira (2004)	Cylinders Spheres Spheres Cylinders Parallellepipiped	Porous ceramic Glass Glass Glass Glass	1.5/3.0/6.3/11.0 3.0 1.5 (length: 3.5) 6 1.9/3.1/4.4 5 (length: 3.5) 2.9×5.5×5.5	34.27/17.13/8.16/4.67 33.33 43.91 ^d 16.67 26.32/16.13/11.36 9.84 ^d 9.07 ^d	51.4 100 100	0.27/0.47/0.87 1 1.7 0.1/0.2/0.3

^aCalculated using $d_{eq}=8.4$ mm reported by the authors.^bSquare cross-section.^cCalculated using $d_{eq}=4.89$ mm and $d_q=8.10$ mm reported by the authors.^dCalculated using d_{eq} defined as the diameter of a sphere having the same volume as the particle.

Table 2: Fluids and operating conditions employed in experimental heat transfer studies in TBR.

Authors	Gas	Liquid	G (kg m ⁻² s ⁻¹)	L (kg m ⁻² s ⁻¹)	Flow regime
Weekman and Myers (1965)	Air	Water	0.07–1.6	1.7–34	Trickle and pulsing ^a
Hashimoto et al. (1976)	Air	Water, aqueous solution and glicerine	0.13–1.4	0.0–32	Trickle, pulsing, and bubbling ^a
Specchia and Baldi (1979)	Air	Water	0.0–1.5	5.6–17.9	LIR and HIR ^a
Matsuura et al. (1979a,b)	Air	Water	0.01–1.1	0.6–50.0	Trickle, pulsing, and bubbling ^a
Crine (1982)	Air	Water	0.007–0.04	1.5–5.0	Trickle ^a
Grosser et al. (1996)	Air	Water and aqueous solution of CMC	Re _c range is reported	Re _l range is reported	LIR and HIR ^b
Lamine et al. (1996)	N ₂	Water/aqueous ETG solution	0.0–0.4	1.0–50.0	LIR and HIR ^a
Babu and Sastry (1999)	Air	Water	0.01–0.898	3.16–71.05	Trickle, pulsing and bubbling ^a
Babu and Rao (2007)					
Babu et al. (2007)					
Mariani et al. (2001)	Air	Water	0.03–0.27	2.38–7.94	Trickle ^a
Borremans et al. (2003)	Air	Water	0.022–0.11	2/4/7	LIR and HIR ^a
Pinto Moreira (2004)	Air	Water	0.0–0.5	2/9/20	Trickle, pulsing, and bubbling ^a

^aDefined by the authors.^bEstimated from experimental data and the Larachi et al. (1993) correlation.

can be solved in terms of the following expression:

$$\frac{T_w - T}{T_w - \bar{T}_0} = 2 \sum_{n=1}^{\infty} \frac{J_0(b_n r / R_t) \exp(-b_n^2 z^*)}{b_n [1 + (b_n / Bi)^2] J_1(b_n)}, \quad (3)$$

where J_0 and J_1 are Bessel functions of the first kind, $Bi = h_w R_t / k_{er}$

$$z^* = \frac{\pi k_{er}}{(Lc_{PL} + Gc_{PG}^*)S} z \quad (4a)$$

and b_n are the positive roots of

$$Bi J_0(b_n) = b_n J_1(b_n). \quad (4b)$$

Two fitting parameters arise from Eqs. (3)–(4b), k_{er} and h_w . This alternative was extensively employed to analyze the thermal behavior of TBR (Hashimoto et al. 1976, Specchia and Baldi 1979, Babu and Sastry 1999, Babu and Rao 2007, Babu et al. 2007).

It is worth mentioning that, in general, the assumption of uniform wall temperature along the tube length has not been experimentally checked because the measure of T_w implies an additional complexity in the experimental set-up. A simpler option, proposed by Mariani (2000), arises by employing conditions at which the temperature of the fluid circulating in the jacket (T_c) remains uniform (i.e., when a phase change takes place or employing a large flow rate). Thus, the boundary condition at the tube wall reads as follows:

$$-k_{er} \frac{\partial T}{\partial r} = h^F [T_c - T(R_t)] \quad \text{at } r=R_t, \quad (4c)$$

$$\text{where } \frac{1}{h^F} = \frac{1}{h_w} + \frac{1}{h_c}. \quad (4d)$$

h^F is a global heat transfer coefficient, while h_c is the jacket heat transfer coefficient, whose value should be independently estimated or measured.

By using $Bi^F = h^F R_t / k_{er}$ instead of Bi and T_c instead of T_w , it is possible to employ the same solution [Eq. (3)]. Besides, the regression will still be performed using two parameters, k_{er} and h^F .

An alternative to a fluid circulating in the jacket as a heat source or sink arises by employing an electrical resistance wound uniformly along the external tube surface (Lamine et al. 1996, Borremans et al. 2003). The power dissipated when an electrical current is passed will be essentially uniform, and in principle, the heat flux received by the bed at the wall, q_c , can also be regarded as being uniform and known. Thus,

$$h_w [T_w - T(R_t)] = -k_{er} \frac{\partial T}{\partial r} = q_c \quad \text{at } r=R_t. \quad (5)$$

A convenient way to evaluate k_{er} at these conditions is by measuring the bed temperature profile at a certain distance z far from the bed inlet, when the fluid flow is uniformly heated all over the cross-section. From Eq. (1) and the second equality in Eq. (5),

$$\frac{dT}{dz} = \frac{2q_c}{(Lc_{PL} + Gc_{PG}^*)R_t}, \quad 0 < r < R_t. \quad (6)$$

With the value of dT/dz in Eq. (6), the radial profile $T(r)$ retrieved from Eq. (1) will depend on k_{er} , which can be calculated by matching with the experimentally measured profile. Afterwards, $T(R_t)$ can be calculated, and by employing the first equality in Eq. (5), h_w can be

estimated, provided that T_w is measured at the same axial position z .

In practice, the condition of uniform q_c along the tube wall is questionable; since the conductivity of the (usually metallic) wall is high, then the wall temperature (T_w) tends to be uniform rather than the flux. The magnitude of this effect will depend on the features of the experimental set-up and experimental conditions. Axial conduction can be reduced by dividing the total length into several sections insulated at the ends.

The inlet condition (2d) has been employed by many authors; however, other alternatives considering a non-uniform temperature profile have been also tried. Pinto Moreira et al. (2006) discussed the effect of a parabolic inlet profile on parameter estimates, following a similar approach with that of Borkink and Westerterp (1992) for single-phase flow. Instead, Mariani (2000) proposed an alternative procedure by considering a generic inlet temperature profile,

$$T = T_0(r) \text{ at } z=0. \quad (7)$$

The solution of Eq. (1), with boundary conditions (2a), (4c), and (4d) and inlet condition (7), leads to

$$\frac{T_c - T}{T_c - T_0(0)} = 2 \sum_{n=1}^{\infty} C_n \frac{J_0(b_n r / R_i) \exp(-b_n^2 y)}{\left[1 + (b_n / Bi^F)^2\right] J_1^2(b_n)}, \quad (8)$$

where

$$C_n = \frac{1}{R_i^2} \int_0^{R_i} \left[\frac{T_c - T_0(r)}{T_c - T_0(0)} \right] J_0(b_n r / R_i) r dr. \quad (9a)$$

In his approach, Mariani (2000) assumed that the bed-axis temperature at the inlet section, $T_0(0)$, is the only measurement required. As in this way the whole profile $T_0(r)$ is not known, an alternative is to adjust as many C_n parameters [Eq. (9a)] as needed to use Eq. (8) in the regression procedure. However, this approach turns out to be impractical if the number of the needed terms in Eq. (8) is large (say, more than 3–4). Mariani (2000) checked that the C_n values for higher-order terms of series in Eq. (8) (i.e., with $n > 1$) are, in practice, considerably lower than C_1 . Therefore, they can be linked with C_1 by assuming that the relationship between C_n and C_1 is the same as the one taking place for uniform inlet temperature [Eq. (3)]:

$$C_n = C_1 \frac{J_1(b_n) b_1}{J_1(b_1) b_n}. \quad (9b)$$

Then, C_1 is included in the set of fitting parameters.

3.2 Adiabatic packed beds

As mentioned in Section 2, Crine (1982) employed a cylindrical packed bed fed with a hot stream in the core region and a cold stream in the annulus. At $r=R_i$, the heat flux is zero,

$$\frac{\partial T}{\partial r} = 0, \quad r=R_i, \quad (10a)$$

while the inlet conditions are

$$T = T_h \quad z=0 \quad 0 \leq r \leq R_i \quad (10b)$$

and

$$T = T_{cd} \quad z=0 \quad R_i \leq r \leq R_i. \quad (10c)$$

R_i is the radius separating the hot and cold streams. The solution of Eq. (1) under conditions (2a) and (10a)–(10c) led to an infinite series, slightly different from Eq. (3) (Crine 1982).

Grosser et al. (1996) used a square cross-section bed fed in each half by cold and hot streams. A heat balance in Cartesian coordinates assuming uniform temperature in the x coordinate for any value of coordinates y and z (axial position), and neglecting the convective transport in the gas stream, was considered:

$$Lc_{pl} \left[\frac{\partial T}{\partial z} \right] = k_{er} \frac{\partial^2 T}{\partial y^2}. \quad (11)$$

It was assumed that small heat penetration depths at both sides of the boundary ($y=0$) between the hot and cold streams took place in the experiments. Then, the following boundary conditions were used:

$$T = T_h \quad y \rightarrow -\infty \quad (12a)$$

and

$$T = T_{cd} \quad y \rightarrow +\infty. \quad (12b)$$

According to the way of feeding streams at the inlet,

$$T = T_h \quad y < 0 \quad z = 0 \quad (12c)$$

and

$$T = T_{cd} \quad y > 0 \quad z = 0. \quad (12d)$$

The solution of Eq. (11) with conditions (12a)–(12d) can be found in Grosser et al. (1996).

3.3 Annular packed bed with heat transfer through the walls

The third experimental set-up described in Section 2 involves heat transfer between the inner and outer walls

of an annular packed bed. Mousazadeh et al. (2012) are the only authors who employed this technique. Unfortunately, they assumed a uniform thermal conductivity without including wall heat transfer coefficients. It was discussed in Section 3.1 that this approach is not suitable for beds of relatively low aspect ratios, as that ($a=10$) studied by Mousazadeh et al. (2012). Therefore, the experimental results from this source will not be further considered in this review.

4 Analysis and discussion of experimental results and literature correlations

4.1 Effective radial thermal conductivity

4.1.1 Literature correlations

The most widely employed approach to correlate k_{er} , according to the 2DPPF model, with operating and geometric variables proposes a polynomial expression that accounts for the contribution of each phase. Nonetheless, there are some works in the literature that have used other approaches.

Larachi et al. (2003) proposed the artificial neural network (ANN) procedure to estimate heat transfer parameters in TBR. *Inputs, outputs, and connectivity weights* to estimate effective radial thermal conductivity can be found in Table 10 of the above-mentioned article; also, it is essential to consult an erratum at the web site <http://www.gch.ulaval.ca/bgrandjean/tbr-pbc/tbr-pbc.html>.

It is worth noting that the ANN correlation provides less physical insight than other expressions that have a stronger phenomenological support. Besides, the database employed should be adequately refined considering experimental information from the same kind of models.

Based on a mechanistic model, Crine (1982) proposed an expression including several parameters to be adjusted from experimental data. He reported values for his experimental conditions employing water and a single particle diameter. As a way to estimate such parameters for different experimental conditions is not provided, this correlation cannot be employed for comparison with experimental values of k_{er} from other sources.

Babu and Rao (2007) proposed an expression for k_{er} involving the identification and adequate combination of heat transfer resistances arising from elementary heat

transfer steps. This approach was previously applied by Dixon (1985) for heat transfer in packed beds with single-phase flow. The main problem in two-phase flow systems is the lack of specific correlations for the large number of parameters that arise. Thus, this approach will not be used for comparative purposes.

Next, the form of the polynomial expressions for k_{er} and the values of their parameters will be revised. In Section 4.1.2, the predictive capabilities of polynomial expressions and the ANN approach through comparisons with available experimental data will be assessed.

Several authors have extended the approach of Yagi and Kunii (1957) for single-phase flow by including the contributions of the two flowing phases in TBR. Then, three contributions to radial thermal conductivity can be identified:

- k_{eo} : thermal conductive contribution
- k_{el} : from liquid flow due to lateral mixing
- k_{eg} : from gas flow due to lateral mixing

Therefore,

$$k_{er} = k_{eo} + k_{eg} + k_{el}. \quad (13)$$

Contributions from the lateral mixing of gas and liquid can be expressed as follows (Ranz 1952):

$$k_{eg} = \alpha_G (\sigma d_p) G c_{pg}^* \quad (14a)$$

and

$$k_{el} = \alpha_L (\sigma d_p) L c_{pl}, \quad (14b)$$

where α_G and α_L are the ratios between mass flow rates in the radial and axial directions. These parameters can vary with liquid and gas flow rate, the thermo-physical properties of fluids, the shape and size of particles, and packing arrangement; and σ is the average distance between neighboring particles measured in particle diameters. As in practice, it is difficult to evaluate α and σ individually, the product ($\alpha\sigma$) is customarily used as a fitting parameter.

Defining $a = \alpha_G \sigma$ and $b = \alpha_L \sigma$ and introducing Re and Pr numbers, Eqs. (14a) and (14b) become

$$k_{eg} = a Re_G Pr_G k_G \quad (15a)$$

and

$$k_{el} = b Re_L Pr_L k_L. \quad (15b)$$

Expressions (15a) and (15b) have been used in a more general form as

$$k_{eg} = a Re_G^c Pr_G^d k_G \quad (16a)$$

and

$$k_{el} = b \text{Re}_L^e \text{Pr}_L^f k_L, \quad (16b)$$

where the exponents c , d , e , and f are also fitting constants.

The following discussion is undertaken with regard to the contribution k_{el} , but the same holds for k_{eg} . The appearance of the molecular thermal conductivity k_L in Eq. (15b) is superfluous, but according to Eq. (16b), it will not be so if $f \neq 1$. Actually, the very nature of the mechanism of lateral dispersion should preclude the effect of k_L . An empirically noticeable effect of k_L on k_{el} may take place at very low values of L when conductive mechanisms [accounted by k_{eo} , according to Eq. (13)] and liquid lateral dispersion are of comparable order of magnitude, and such effect will therefore respond to a correction to the assumption of additive contributions in Eq. (13). In any case, the effect is expected to vanish when $k_{el} > k_{eo}$, at higher values of L , but if $f \neq 1$, this can only happen by a countereffect of k_L casted in b . As discussed below, some correlations employ $f \neq 1$, but no effect of k_L in b is included.

In the following paragraphs, the way in which each contribution has been considered by different authors will be analyzed. In general, the most significant contribution is the one from the flow of liquid phase, k_{el} . Then, it is not surprising that some authors have explicitly disregarded the other two. Another aspect that should be mentioned concerns the flow regime. In general, despite the fact that several flow regimes can be found in practice (Saroha and Nigam 1996), for the sake of heat transfer correlations, just a simple distinction between low-interaction regime (LIR) and high-interaction regime (HIR) has normally been made.

The parameter k_{eo} in Eq. (13) should account for conductive mechanisms in the particle, gas, and liquid phases. Both fluid phases participate according to their volume fractions in the interstitial voids left by the packing (i.e., according to the liquid saturation, β_L). As such volume fractions depend, in particular, on the flow rates of both fluids, it is expected that k_{eo} will depend on the actual operating conditions. However, it should be noted that in the literature, k_{eo} is most frequently referred to as the “stagnant contribution”. This term may be somewhat misleading, as “stagnant” suggests conditions without fluid flow, at which β_L can be very different from the operating value.

Theoretical and semiempirical expressions have been proposed to estimate k_{eo} . Thus, Specchia and Baldi (1979) suggested the following expression:

$$\frac{k_{eo}}{k_G} = \left[\varepsilon + \frac{1-\varepsilon}{0.22 \varepsilon^2 + 2k_G / (3k_S)} \right]. \quad (17)$$

This expression assumes that the voids are just occupied by the gas phase ($\beta_L=0$), and therefore, low values of k_{eo} will be predicted.

Chu and Ng (1985) obtained the following theoretical expression from the application of the effective medium theory:

$$k_{eo} = \frac{\Phi + [\Phi^2 + 8\psi k_G k_L]^{1/2}}{4\psi}, \quad (18a)$$

where

$$\Phi = [2 - 3(1 - \varepsilon + \varepsilon\beta_{LD})] \psi k_G + [3(1 - \varepsilon + \varepsilon\beta_{LD}) - 1] k_L \quad (18b)$$

and

$$\psi = \frac{\zeta^3(k_S + 2k_L) - (k_S - k_L)}{\zeta^3(k_S + 2k_L) + 2(k_S - k_L)}, \quad \zeta = \left[1 + \frac{\beta_{LD} \varepsilon}{(1 - \varepsilon)} \right]^{1/3}. \quad (18c)$$

In Eqs. (18), β_{LD} is the dynamic liquid saturation, for which the authors suggested the use of the Wijffels et al. (1974) correlation:

$$\beta_{LD} = \left[\left(\frac{200}{\text{Re}_L} + 1.75 \right) \frac{L^2}{g d_p \rho_L^2} \frac{(1-\varepsilon)}{\varepsilon^3} \right]^{1/4}.$$

It is worth mentioning that Chu and Ng (1985) pointed out that Eq. (18a) is accurate only for values of the ratios k_S/k_G and k_S/k_L of less than about 10.

Mariani (2000) proposed a modification of the well-known Bauer and Schlünder (1978a) expression for single-phase flow, assuming that the liquid occupies the empty space between contacting particles and the rest of the interstitial volume is filled by the gas phase. As the effect of the liquid phase may be, in this way, overestimated, the predictions of Mariani's correlation may be regarded as representing an upper bound for k_{eo} . The following expression results:

$$k_{eo} = (1 - \sqrt{1 - \varepsilon}) k_G + \sqrt{1 - \varepsilon} \Theta k_L, \quad (19a)$$

where

$$B = C_f \left(\frac{1-\varepsilon}{\varepsilon} \right)^{10/9}; \quad N = 1 - \frac{B}{\kappa}; \quad \kappa = \frac{k_S}{k_L}; \quad (19b)$$

and

$$\Theta = \frac{2}{N} \left\{ \left(\frac{B(\kappa-1)}{N^2 \kappa} \right) \ln \left[\frac{\kappa}{B} \right] - \frac{B+1}{2} - \frac{B-1}{N} \right\}. \quad (19c)$$

B is the deformation factor. For spheres of the same size, $C_f=1.25$.

The contribution k_{eg} has been disregarded by Chu and Ng (1985), Grosser et al. (1996), Lamine et al. (1996), Mariani et al. (2001), and Pinto Moreira (2004). The authors who maintained this term have assumed $c=d=1$ in Eq. (16a). Instead, parameter a changes in the different

sources. Hashimoto et al. (1976) proposed $a=0.095$, while Matsuura et al. (1979a) evaluated different values that can be correlated with particle size as $a=0.43 d_p^{0.275}$ (d_p in mm). Specchia and Baldi (1979) employed an expression that depends on the aspect ratio a , $a=1/[8.65(1+19.4/a^2)]$. Babu et al. (2007) used different values of a ranging from 0.11 to 0.13 depending on particle shape and size.

The contribution k_{el} was considered in all studies. Table 3 presents expressions or values for parameters b , e , and f in Eq. (16b). In all correlations for k_{el} , at least one parameter was obtained by fitting experimental data, except the one by Chu and Ng (1985), which was developed theoretically from the random walk theory.

The comparison of correlations for k_{el} allows drawing some useful conclusions (Table 3). Specchia and Baldi (1979) and Lamine et al. (1996) presented different

expressions for HIR and LIR, while Hashimoto et al. (1976), Matsuura et al. (1979a), Pinto Moreira (2004), and Babu et al. (2007) employed a single correlation. Nonetheless, when fluid-dynamic parameters (e.g., liquid saturation β_L) should be calculated, a distinction between flow regimes is implicitly made. In almost all correlations, the power e in Re_L^e is bounded as $0.6 < e < 1$, except for Specchia and Baldi's correlation, in which it is < 0.33 . Finally, the values adopted for parameter f in Eq. (16b) deserve a comment. In some correlations, despite that a single liquid was used in the experiments, $f=1$ is fixed according to Eq. (15b). In other cases (e.g., Pinto Moreira 2004), $f=0$ in Eq. (16b) is taken and, therefore, parameter b becomes strictly valid for the specific fluid used in the experiments. An atypically low dependence of k_{el} on Pr_L ($f=0.2$) is proposed by Grosser et al. (1996).

Table 3: Expressions for parameters of k_{el} [Eq. (16b)].

Authors	Regime			
		b	e	f
Hashimoto et al. (1976) ^a	LIR/HIR	$\left\{ 0.197 + \frac{1}{1.9 + 0.0264 [d_{eq} L / (\varepsilon \beta_L \mu_L) (\mu_L / \mu_0)]} \right\} \frac{d_{eq}}{d_p}$	1	1
Specchia and Baldi (1979) ^b	LIR	$24.4 (\varepsilon \beta_L)^{0.87}$	0.13	1
	HIR	$\frac{0.003}{(\varepsilon \beta_L)^{0.29}} \left[\frac{a_v d_p}{\varepsilon} \right]^{2.7}$	0.325	1
Matsuura et al. (1979a)	LIR/HIR	$0.2084 d_p^{-0.2207} [1 + 0.0492 \exp(-0.4821 d_p) Re_G]$	1	1
Chu and Ng (1985)	LIR	0.167	1	1
Lamine et al. (1996)	LIR	$\frac{1}{8 \beta_L \left[2 - \left(1 - \frac{2}{a} \right)^2 \right]}$	1	1
	HIR	$1.76 \beta_L^{2/3}$	2/3	2/3
Grosser et al. (1996)	HIR	$\frac{2.1}{(1-\varepsilon)^{0.57}} Re_G^{-0.13}$	0.7	0.2
Mariani et al. (2001)	LIR	$0.281 (1 + 5.3 \cdot 10^{-3} Re_G)$	0.81	1
Pinto Moreira (2004) ^c	LIR/HIR	$7.59 \frac{\beta_L^{0.7} (d_{eq}/d_t)^{0.08}}{(Z/d_t)^{0.51} \phi^{0.16} k_L}$	0.62	0
Babu et al. (2007) ^b	LIR/HIR	$0.928 \varepsilon^{0.379} \beta_L^{0.342} (1 - \beta_L)^{0.037} a_v^{0.008} Re_G^{-0.037}$	0.658	1

$$^a d_{eq} = \frac{2}{3} \frac{\varepsilon}{1-\varepsilon} d_p.$$

$$^b a_v = \frac{6(1-\varepsilon)}{d_p}.$$

$$^c d_{eq} = \left(\frac{6 V_p}{\pi} \right)^{1/3}; \phi = 6 V_p / d_{eq} S_p.$$

4.1.2 Analysis of the available experimental information and correlations for radial effective thermal conductivity

To analyze the performance of the different literature correlations, it is first necessary to have available a refined database. According to Tables 1 and 2, most of the experimental information was obtained using air and water as fluids and beds packed with spheres. Therefore, the alluded database and the analysis undertaken in the present section and in Sections 4.1.3 and 4.1.4 will be restrained to these conditions, while the scarcer data under other different conditions will be discussed in Section 4.1.5. The database includes results from Hashimoto et al. (1976), Matsuura et al. (1979a), Crine (1982), Colli Serrano (1993), Lamine et al. (1996), Mariani (2000), and Borremans et al. (2003). Data from other sources in Table 1 have not been considered for different reasons exposed previously or in the remainder of this section. As such, the experimental results of Babu and coworkers (Babu and Rao 2007, Babu et al. 2007) cannot be included due to the fact that conditions for individual data points have not been reported.

It is worth commenting that packing procedure (Zou and Yu 1995) and start-up operation (Loudon et al. 2006, Joubert and Nicol 2009) may also influence thermal conductivity values, but no systematic studies were found in the literature to undertake a reliable analysis.

4.1.2.1 Thermal conductive contribution

Aiming to discuss the relevance of the stagnant contribution to k_{er} , the available experimental results will be employed. First, it should be noted that Grosser et al. (1996) and Pinto Moreira (2004) neglected k_{eo} , while Lamine et al. (1996) did not explain how k_{eo} was evaluated.

The value of k_{eo} estimated by Hashimoto et al. (1976) from their experimental data for glass spheres is 0.465 W/mK. Under their experimental conditions, this value of k_{eo} represents <7% of k_{er} , decreasing significantly as liquid flow rate is increased. Similarly, Matsuura et al. (1979a) reported values of k_{eo} between 0.81 and 1.05 W/mK, depending on the particle size. In this study, a very large range of L was tested, and for the lowest values of L , the contribution of k_{eo} reached around 35%.

Using Eq. (19a) as a reference, a value $k_{eo}=0.764$ W/mK is predicted for the conditions in the study of Hashimoto et al. (1976), compared to their experimental value of 0.465 W/mK, while for the experiments of Matsuura et al. (1979a), $k_{eo}=0.717$ W/mK is predicted against the experimental range 0.81–1.05 W/mK. Reasonable values arise

from Eq. (19a), despite that it has been regarded as providing upper estimates. For experimental conditions in other contributions, values of k_{eo} from Eq. (19a) are always <1 W/mK.

Some facts about stagnant thermal conductivity can be gathered from the previous analysis:

- The contribution of k_{eo} to k_{er} cannot be ignored without a previous analysis, particularly in trickle regime at low flow rates (frequently employed in laboratory TBR).
- k_{eo} can be considered negligible for high water-liquid flow rates. Nonetheless, for liquids having higher viscosities or lower specific heats than water, this contribution can be more important.

4.1.2.2 Effect of geometric features of the packed bed: particle diameter and aspect ratio

In general, thermal conductivity depends on both particle (d_p) and tube (d_t) diameter. The effect of tube diameter is suitably accounted for in terms of the aspect ratio a .

In principle, the wall effects can exert an influence on k_{er} , which, therefore, should vanish at high values of a (tentatively, $a>15$). Actually, this behavior is observed from the values of k_{er} reported by Crine (1982) and Grosser et al. (1996). However, to our knowledge, no systematic analysis about the effect of a has been performed in TBR. Consequently, most correlations to estimate k_{er} (see Table 3) do not include an explicit dependence on a . Two exceptions can be mentioned. For the LIR, Lamine et al. (1996) introduced the effect of a in k_{el} in the same way as Bauer and Schlünder (1978b) did for single-phase flow. As a result, k_{el} increases as a is increased, reaching an asymptotic value. Pinto Moreira (2004) proposed $k_{el} \propto a^{0.43}$, which does not present an adequate physical support, as k_{el} would increase boundlessly with a . When comparing such estimations with experimental data from Crine (1982), obtained in a bed of large aspect ratio, systematic overestimations (around 67%) arise, while noticeable underestimations (around 34%) are found with respect to the results of Borremans et al. (2003), obtained in a packed bed with a relatively small a .

According to Eqs. (14a) and (14b) and taking into account that the k_{eo} is almost negligible in Eq. (13) for most of the available experimental results, it can be expected that k_{er} will linearly increase with d_p , provided that results at high enough values of a , to avoid wall effects, are considered. In the following examples, care has been taken to fulfill this requirement. The results from Hashimoto et al. (1976) for a d_p ratio of 1.85 roughly confirm this trend, as can be observed in Figure 1. Continuous lines, obtained using Eq. (22) for LIR and Eq. (24) for HIR, will

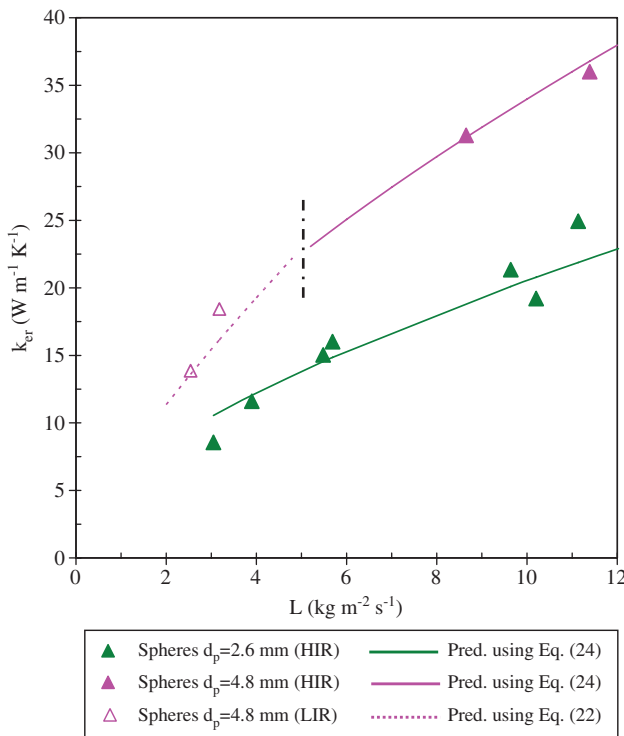


Figure 1: k_{er} vs. L for spheres of different d_p ($d_t=0.0738$ m, $Re_g=34.79$).

Symbols: experimental data from Hashimoto et al. (1976).

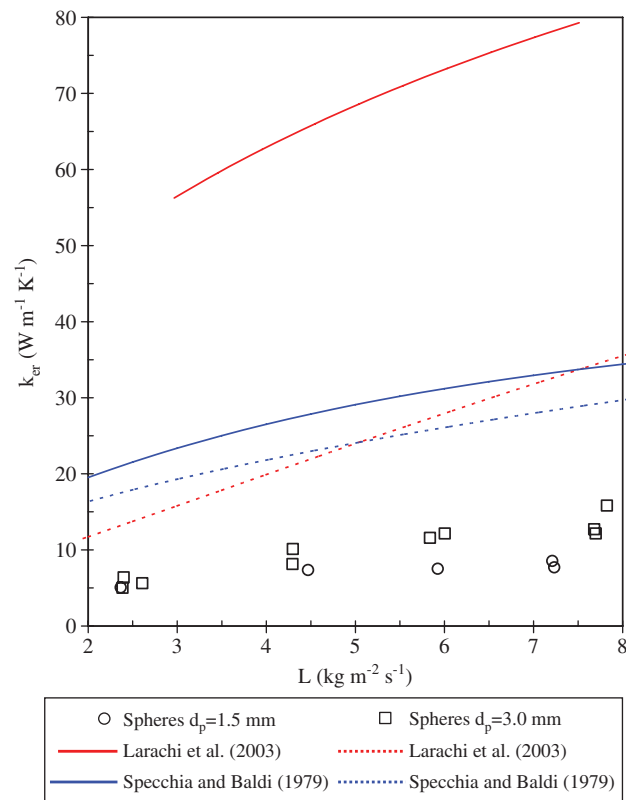


Figure 2: k_{er} vs. L for different d_p ($d_t=0.0514$ m, $Re_g=4.3$).

Symbols: experimental data from Mariani et al. (2001).

be discussed in Section 4.1.4. The data of Mariani et al. (2001) show a somewhat weaker effect of d_p , although a definitely increasing trend can be appreciated in Figure 2. The correlations of Specchia and Baldi (1979) and Larachi et al. (2003) predict the opposite effect of d_p on k_{er} , as illustrated in Figure 2. Thus, these two correlations cannot be considered reliable for estimation purposes. For the same reason, the experimental results from Specchia and Baldi (1979) have been not included in the refined database discussed at the beginning of this section.

4.1.2.3 Operating condition: effect gas and liquid flow rates

The effect of gas (G) and liquid (L) superficial mass flow rates was studied by almost all the authors.

All sets of experimental data show that k_{er} increases as L is increased (e.g., Figures 1 and 2), a general trend that is supported mechanistically by Eq. (15b). Despite the fact that most of the correlations reproduce this behavior, the magnitude of the impact of L on k_{er} differs significantly (Table 3).

Although according to Eqs. (13) and (14), the effect of G is expected to be similar to that of L , only a mild impact

is found in practice. This is most probably due to the fact that usual values of G are definitely much lower than L (see Table 2), and therefore, the contribution of k_{eG} on k_{er} becomes masked by high values of k_{el} .

Most of the correlations predict a low effect of G , as illustrated in Figure 3, with the exceptions of those of Matsuura et al. (1979a) and Larachi et al. (2003), which show an unusual significant effect of G . In addition, it can be observed from Table 3 that, in some correlations, the effect of G is included in parameter b of k_{el} .

It is worth mentioning that there are no experimental studies at high pressure, which affects fluid dynamics and probably k_{er} .

4.1.3 Comparison of prediction of available correlations with the experimental database

The previous analysis allows disregarding some correlations for k_{er} due to the fact that they predict an inconsistent effect of some operating or geometric variables. To assess the predictive capability of the remaining expressions, their estimations will be compared with the refined

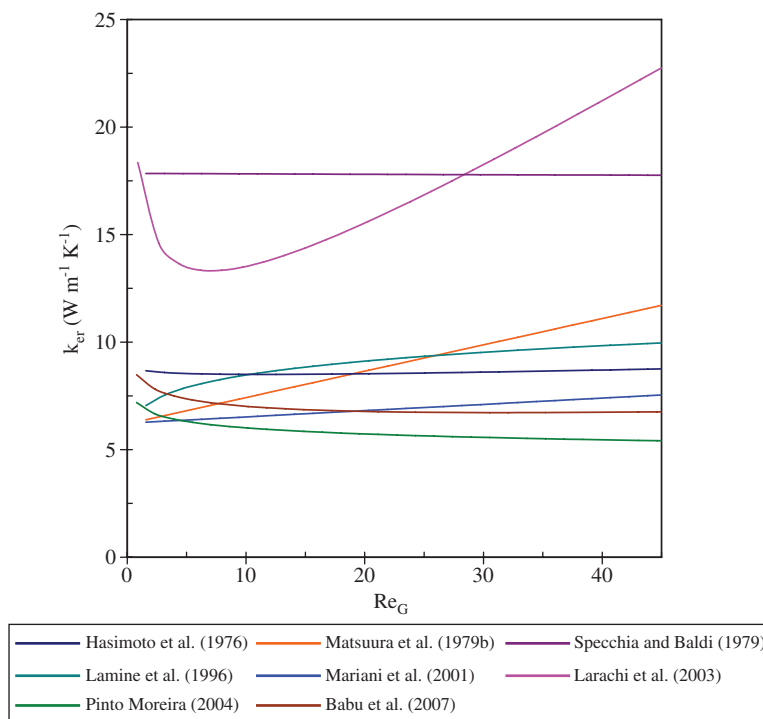


Figure 3: k_{er} vs. Re_G in LIR (from correlations in Table 3; air and water, $d_t=0.0514$ m, $d_p=0.003$ m, $Re_L=10.9$).

database (Section 4.1.2). These data have been classified according to the fluid-dynamic regimes in two groups corresponding to LIR and HIR by using the correlation of Larachi et al. (1993). Nonetheless, in account of the transition regime – not considered by such correlation – some results pertaining to HIR, but close to the boundary, were included in both groups.

For the LIR group, 128 experimental values of k_{er} from Hashimoto et al. (1976), Matsuura et al. (1979a), Crine (1982), Lamine et al. (1996), Mariani (2000), and Borremans et al. (2003) were collected. Full experimental conditions provided in these sources allow a direct comparison with correlations estimates. The six correlations tested (Hashimoto et al. 1976, Matsuura et al. 1979a, Chu and Ng 1985, Lamine et al. 1996, Mariani et al. 2001, Babu et al. 2007) show average relative errors defined as

$$\varepsilon = \frac{\sum_{i=1}^N \left| \left(k_{er,i}^{pred} - k_{er,i}^{exp} \right) / k_{er,i}^{exp} \right|}{N} \cdot 100 \quad (20)$$

between 20 and 30%. The correlations of Hashimoto et al. (1976), Lamine et al. (1996), and Mariani et al. (2001) present the lowest deviations.

The HIR group includes 221 values of k_{er} reported by Hashimoto et al. (1976), Matsuura et al. (1979a), Colli Serrano (1993), Lamine et al. (1996), and Borremans et al.

(2003). Out of the five correlations tested (Hashimoto et al. 1976, Matsuura et al. 1979a, Grosser et al. 1996, Lamine et al. 1996, Babu et al. 2007), the one by Lamine et al. (1996) leads to the best predictions ($\varepsilon=15.4\%$), with an acceptable error balance (140 positive and 79 negative). Deviations of the remaining four correlations range from 23 to 39%.

It should be mentioned that the results from Grosser et al. (1996) were initially included, but this data set was not consistent with the remaining experimental set.

4.1.4 New correlations

From the results of the previous analysis and having available a larger database than the sets of experimental values used to generate each correlation of Table 3, two new correlations based on Eqs. (13) and (16) to predict k_{er} for LIR and HIR regimes are proposed.

For LIR, the contribution k_{eG} in Eq. (13) was disregarded, as preliminary tests using Eq. (14a) show no statistical significance for the effect of G . k_{e0} was estimated using Eq. (19a) and k_{el} was expressed as in Eq. (16b), but including a dependence of coefficient b with β_L in the form $b=b^*\beta_L^{-p}$, with β_L evaluated from the Larachi et al. (1991) correlation. Although only experiments using water were considered, $f=1$ was assumed in the term

\Pr_L^f of Eq. (16b), following the discussion in Section 4.1.1 about the effect of k_L .

$$k_{er} = k_{eo} + b^* \beta_L^p Re_L^e \Pr_L k_L \quad (21)$$

The fitting parameters were b^* and the exponents p and e . The results obtained for the exponents were quite close to 1 ($p=0.94$, $e=0.98$), and therefore, it was decided to assume directly that $p=e=1$. Actually, $e=1$ corresponds to the original theory of Ranz (1952) [see Eqs. (15b) and (16b)]. The experimental data were then reanalyzed to fit the only parameter left, b^* . In this way, the following expression was finally reached, with $b^*=0.093$:

$$k_{er} = k_{eo} + 0.093 \left(\frac{Re_L \Pr_L}{\beta_L} \right) k_L = k_{eo} + 0.093 \left(\frac{L}{\beta_L} \right) d_p c_{pl}. \quad (22)$$

Expression (22) fits the experimental results with a relative average error of 17.8% and shows a reasonably balanced error distribution (77 positive and 53 negative values). The average error is virtually the same as that originally arisen by using Eq. (21). Figure 4 shows a parity plot for k_{er} in LIR, as estimated from Eq. (22). The sources of experimental data are displayed in Figure 4.

It is noted that L/β_L is a modified superficial mass liquid velocity excluding the fraction of voids occupied by the gas phase. It is also interesting to remark that the coefficient $b^*=0.093$ is quite similar to that in the very well-known correlation of Yagi and Kunii (1957) for one-phase flow ($b^*=0.1$).

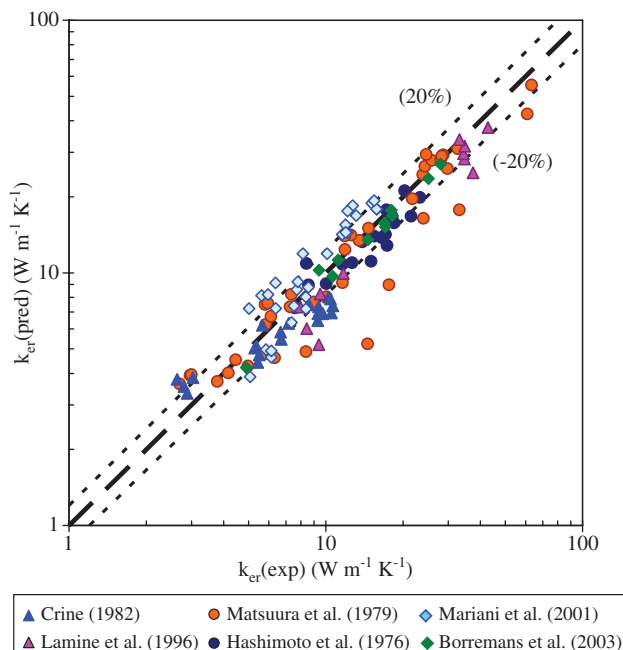


Figure 4: Parity plot between experimental and predicted [using Eq. (22)] values of k_{er} in LIR.

Eq. (22) is valid for the following conditions (air and water):

$$\begin{aligned} 1.5 &\leq d_p (\text{mm}) \leq 6 \\ 15 &< a \\ 4.2 &\leq Re_L \leq 90 \\ 0.000+6 &\leq L/\rho_L (\text{m/s}) \leq 0.02 \\ 0.21 &\leq Re_G \leq 300 \end{aligned}$$

Although the contribution k_{eg} was not significant in LIR, as discussed before, it is worth noting that some effect of G is still noticeable, with regard to the estimation of β_L according to the Larachi et al. (1991) correlation.

To develop a correlation for HIR, the starting point was to consider an expression similar to Eq. (21). Nonetheless, a preliminary analysis indicated that G shows an effect upon k_{el} . Hence, the modified expression undertaken for the regression analysis was

$$k_{er} = k_{eo} + b^* \beta_L^p Re_G^g Re_L^e \Pr_L k_L. \quad (23)$$

Values of k_{eo} and β_L were evaluated as for LIR analysis. The best values of the fitting parameters were $b^*=0.077$, $p=2.14$, $g=-0.23$, $e=1.00$. Therefore, the proposed correlation becomes

$$\begin{aligned} k_{er} &= k_{eo} + 0.077 \beta_L^{2.14} Re_G^{-0.23} Re_L \Pr_L k_L \\ &= k_{eo} + 0.077 \beta_L^{2.14} Re_G^{-0.23} \left(\frac{L}{\beta_L} \right) d_p c_{pl}. \end{aligned} \quad (24)$$

Eq. (24) is valid for the following conditions (air and water):

$$\begin{aligned} 2.6 &\leq d_p (\text{mm}) \leq 6 \\ 15 &< a \\ 12 &\leq Re_L \leq 450 \\ 0.0022 &\leq L/\rho_L (\text{m/s}) \leq 0.05 \\ 0.21 &\leq Re_G \leq 350 \end{aligned}$$

A parity plot for k_{er} in HIR is presented in Figure 5. The average relative error is 9.9%, with 121 positive and 98 negative values.

It is worth mentioning that, according to Eq. (24), k_{er} can increase or decrease with G depending on the values of the remaining variables. This is due to the fact that β_L decreases when G increases, according to the Larachi et al. (1991) correlation. Nonetheless, G exerts a definitely weaker effect than L does.

Figure 1 shows a set of experimental data from Hashimoto et al. (1976), which span over both LIR and HIR. Estimates from Eqs. (22) and (24) included in Figure 1 indicate that the new correlations are able to capture the effect of particle diameter and liquid flow rate.

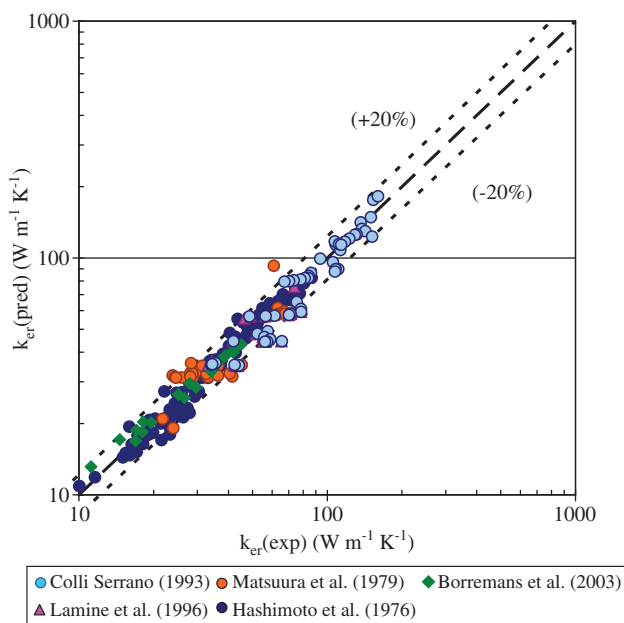


Figure 5: Parity plot between experimental and predicted [using Eq. (24)] values of k_{er} in HIR.

4.1.5 Experimental studies with other fluids and different particle shapes

The discussion in Sections 4.1.2 to 4.1.4 was limited to systems packed with spherical particles and employing air and water. In the following section, studies involving other fluids and/or other particle shapes will be considered.

4.1.5.1 Fluids different from air and water

According to Table 2, no gas other than air and N_2 were employed in heat transfer studies in TBR. Available correlations can be used as a first approximation, considering that the effect of the gas flow rate is of little significance.

Concerning thermal liquid properties, k_l will influence mainly through k_{eo} , and therefore, a very modest impact of this property can be expected (the discussion in Section 4.1.1 is recalled). Instead, c_{pl} will exert a significant effect on the dominant contribution k_{el} [see Eq. (14b)], in a nearly linear way. On the other hand, viscosity, density, surface tension, and liquid-solid interfacial tension will also present some effect on k_{el} . According to Eq. (16b), these properties can show an effect through parameter b . A further dependence on μ_l will arise from the product $Re_L^e Pr_L^f$, if $e \neq f$.

Only a few studies employing aqueous solutions (see Table 2) instead of water can be found in the literature. Hashimoto et al. (1976) compared results employing water and an aqueous solution of glycerin. A moderate

influence of the type of liquid on k_{er} was observed, which was ascribed to an effect of μ_l on parameter b in Eq. (16b), as $e=f=1$ was assumed (see also Table 3).

Grosser et al. (1996) performed experiments using water and an aqueous carboxymethyl cellulose (CMC) solution, intending to modify μ_l . Their data in HIR show higher values of k_{er} for water, a result that was interpreted by the effect of μ_l according to $Re_L^{0.7} Pr_L^{0.2} k_L$ (see Table 3). Clearly, a noticeably low exponent of Pr_L , $f=0.2$, was employed, which is not backed up by other correlations or experimental results. In this way, their expression also predicts $k_{el} \propto k_L^{0.8}$, which can hardly be supported for a lateral dispersion mechanism (see also discussion in Section 4.1.1).

Lamine et al. (1996) employed water and a 40% ethylene glycol (ETG) aqueous solution. They did not find a significant difference between the behaviors of both fluids in LIR, but in accordance to Grosser et al. (1996), k_{er} was found to be larger for water than for the more viscous ETG solution.

In summary, no generally accepted conclusions about the influence of the liquid phase properties on k_{er} have been reached. Thus, further experimental studies are necessary to understand and quantify these effects.

4.1.5.2 Different particle shapes

Particle geometries different from spherical are frequently employed in TBR. In spite of this fact, just a few experimental heat transfer studies including nonspherical particles have been carried out, as can be seen in Table 1.

Specchia and Baldi (1979) reported that k_{er} for Raschig rings was larger than for spheres when compared at the same equivalent diameter. The authors proposed for HIR a single correlation for spheres and rings, which includes a term that accounts for particle shape. However, recalling that their correlation could not be considered reliable for spheres (see Section 4.1.2), it cannot be recommended for other shapes either.

From the PhD dissertation of Pinto Moreira (2004), Figure 6 shows the results of k_{er} vs. G , covering different fluid-dynamics regimes, for three particle shapes (spheres, cylinders, and parallelepipeds). It can be observed that k_{er} diminishes as sphericity increases.

Babu et al. (2007) employed spheres and Raschig rings of different sizes in their experimental study, but the influence of particle shape cannot be inferred from the reported results.

Spheres and porous cylinders of a single size were used by Borremans et al. (2003). The authors just reported experimental result without proposing any correlation. Aiming at fitting the experimental data for cylinders from

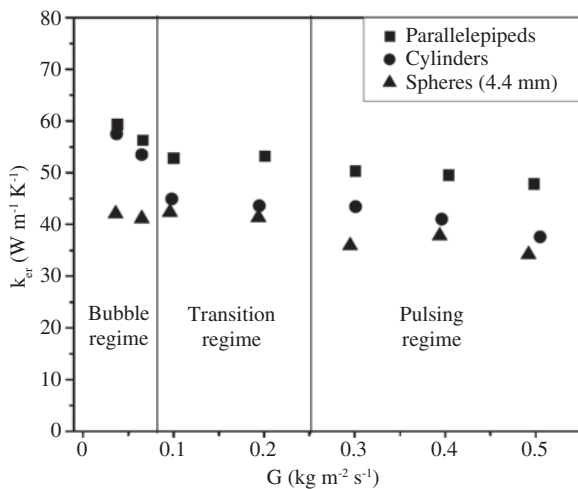


Figure 6: k_{er} vs. G for different particle shapes (sphere, cylinder, and parallelepiped) having the same equivalent diameter ($L=20 \text{ kg m}^{-2} \text{ s}^{-1}$).

Borremans et al. (2003), an expression analogous to Eq. (22) is proposed:

$$k_{er} = k_{eo} + 0.104 \left(\frac{Re_L Pr_L}{\beta_L} \right) k_L = k_{eo} + 0.104 \left(\frac{L}{\beta_L} \right) d_{eq} c_{pl}, \quad (25)$$

where the coefficient 0.104 was fitted and d_{eq} is defined as the diameter of a sphere having the same volume as the cylinder; $k_{eo}=1.05 \text{ W/mK}$ was adopted and β_L has been calculated using the Larachi et al. (1991) correlation.

A satisfactory fitting of experimental data from Eq. (25) is achieved (average relative error: 4.5%), as can be appreciated in Figure 7. However, it should be borne in mind that the number of available experimental points is low. It can be observed that Eqs. (22) and (25) differ slightly by the value of the numerical coefficients, 0.093 and 0.104, as can be appreciated in Figure 8.

It is worth noting that multilobular particles, widely employed in several processes carried out in TBR, have not been employed in experimental studies.

4.2 Wall heat transfer coefficient

There are different difficulties in estimating h_w . On one hand, this parameter does not describe a single feature, but it encloses a number of effects related to changes in particle packing and fluid flow in the near-wall region, as discussed extensively in Dixon (2012) for one-phase flow and specifically for TBR in Mariani et al. (2001).

On the other hand, the relevance of h_w in the global heat transfer process is revealed at relatively low aspect ratios a . Otherwise, the overall heat transfer resistance is dominated by that of the bed core, i.e., R_t/k_{er} . Thus, for a

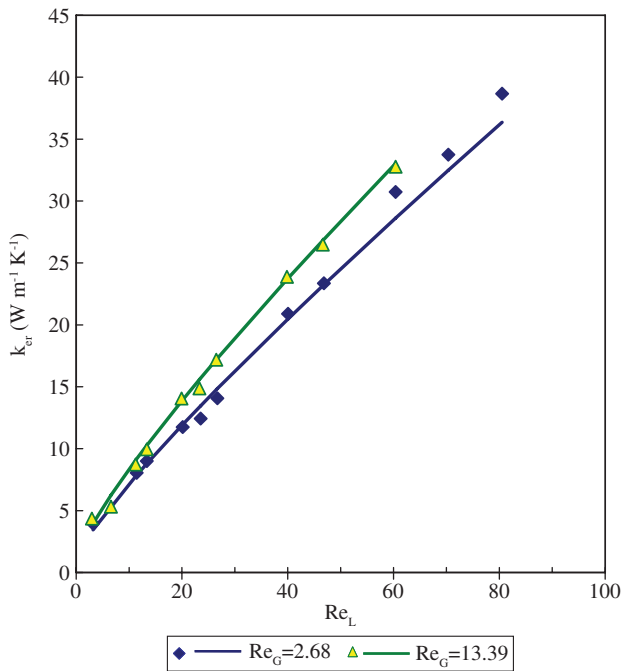


Figure 7: k_{er} vs. Re_L for cylindrical particles.
Symbols: experimental data from Borremans et al. (2003). Continuous lines: predictions from Eq. (25).

meaningful determination of h_w , low values of a should be employed. This aspect has not been adequately considered in some of the literature studies reporting values of h_w .

4.2.1 Available correlations

The purpose of this section is to summarize available literature correlations.

Muroyama et al. (1977) proposed two different expressions according to Re_L :

for $4 < Re_L (\mu_L / \mu_{L0}) < 30$,

$$Nu_w = \frac{h_w \cdot d_p}{k_L} = 0.012 Re_L^{1.7} Pr_L^{1/3}, \quad (26a)$$

and

for $30 \leq Re_L (\mu_L / \mu_{L0}) < 200$,

$$Nu_w = \frac{h_w \cdot d_p}{k_L} = 0.092 \left(\frac{Re_L}{\epsilon \beta_L} \right)^{0.8} Pr_L^{1/3}, \quad (26b)$$

where μ_L and μ_{L0} are liquid viscosities at bed average temperature and at 15°C, respectively.

Matsuura et al. (1979b) presented a model distinguishing five mechanisms to heat transfer in the vicinity of the wall, which leads to the following equation:

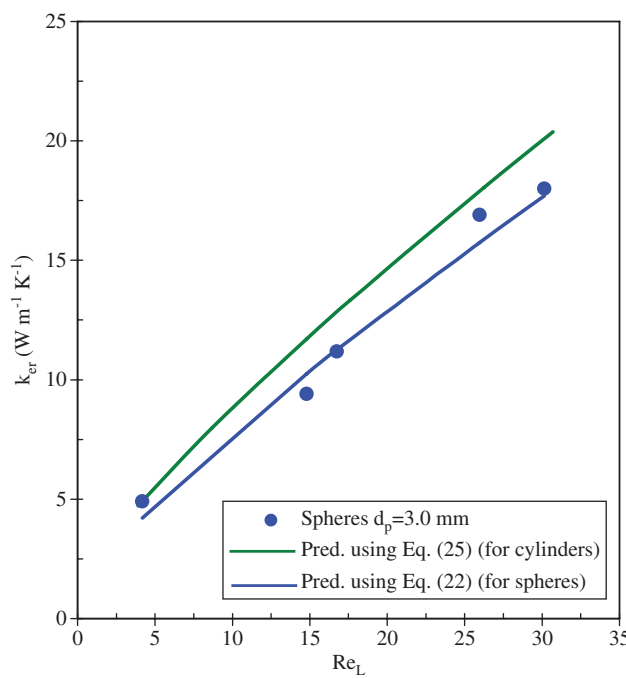


Figure 8: k_{cr} vs. Re_L for a sphere and a cylinder of the same equivalent diameter ($d_{eq}=3$ mm, $Re_g=13.39$).

Experimental data for spheres from Borremans et al. (2003).

$$h_w = h_{w0} + h_{ws} + \frac{1}{\frac{1}{h_{wt,L}} + \frac{1}{h_{wt,G}} + \frac{1}{h_w^*}}, \quad (27)$$

where coefficients account for the following mechanisms:

- Heat transfer through solid-solid contact between particles and the wall surface, h_{w0}
- Heat transfer through liquid around contact points, h_{ws}
- Heat transfer due to lateral liquid flow, $h_{wt,L}$
- Heat transfer due to lateral gas flow, $h_{wt,G}$
- Heat transfer through fluid film on the container wall, h_w^*

Matsuura et al. (1979b) recognize that it is quite difficult to obtain the dependence of each coefficient in Eq. (27) on operating conditions, thermophysical properties, and packing features just from experimental data of h_w . To deal with this scenario, the authors made some assumptions. h_{ws} and h_{w0} are evaluated as explained below. To estimate the remaining coefficients, it was considered that in LIR, the liquid does not intrude into the wall zone, and therefore, $h_{wt,L}=0$ and a film of pure gas covers the wall. Then, h_w^* and $h_{wt,G}$ are evaluated from single (gas) phase correlations. On the contrary, for HIR, the opposite assumption is taken (i.e., absence of gas in the wall zone) and then $h_{wt,G}=0$ and h_w^* and $h_{wt,L}$ are evaluated from single (liquid) phase correlations.

h_{w0} was obtained by extrapolation of the experimental results at no-flow condition and h_{ws} was correlated as a function of liquid dynamic saturation (under the assumption that liquid is present around the contact points) by distinguishing between LIR and HIR conditions.

No physical explanation or experimental evidence (i.e., liquid distribution measurements) was provided by Matsuura et al. (1979b) to support the hypothesis of the absence of liquid on the wall in LIR. On the contrary, it has already been demonstrated by Weekman and Myers (1964) and Mariani et al. (2005) that in the trickle regime (i.e., LIR), the liquid flow in the wall region is always higher than that in the bed core. Thus, an uneven liquid distribution takes places, but in the opposite sense to that stated by Matsuura et al. (1979b).

Specchia and Baldi (1979) indicated that values of h_w in TBR are at least an order of magnitude larger than those for single gas flow in packed beds because of the existence of a liquid film at the wall. For LIR, the authors postulated a dependence of h_w on liquid interstitial velocity through the following expression:

$$Nu_w = \frac{h_w \cdot d_p}{k_L} = 0.057 \left(\frac{Re_L}{\varepsilon \cdot \beta_L} \right)^{0.89} Pr_L^{1/3}. \quad (28)$$

A nearly constant value of h_w irrespective of gas and liquid flow rates, and size, and shape of particles was reported by Specchia and Baldi (1979) for HIR:

$$h_w = 2100 \text{ (W m}^{-2} \text{ °C}^{-1}\text{).} \quad (29)$$

Lamine et al. (1996) presented an empirical dimensional expression for HIR,

$$h_w = 318 \beta_L L \text{ [W m}^{-2} \text{ °C}^{-1}\text{].} \quad (30)$$

For LIR, Mariani et al. (2001) proposed the following correlation:

$$Nu_w = \frac{h_w \cdot d_p}{k_L} = Nu_{w0} + 0.471 Re_L^{0.65} Pr_L^{1/3}, \quad a > 15, Re_L < 40. \quad (31a)$$

Nu_{w0} is a stagnant Nusselt number that can be estimated following the procedure proposed by Mariani (2000). A simplified expression for spheres of diameter between 1.5 and 6 mm is

$$Nu_{w0} = 1.8 - 81 d_p [\text{m}]. \quad (31b)$$

Pinto Moreira (2004) suggested a single correlation irrespective of flow regime:

$$Nu_w = \frac{h_w \cdot d_{eq}}{k_L} = 0.29 \left(\frac{Re_L}{\phi \cdot \beta_L} \right)^{0.77} \left(\frac{Z}{d_t} \right)^{-0.32}, \quad (32)$$

where d_{eq} is the equivalent diameter (defined as the diameter of a sphere of the same volume as the particle) and ϕ is the sphericity ($=6V_p/d_{eq}S_p$). Re_L should be calculated using d_{eq} .

As the expression proposed by the authors to estimate k_{er} (Table 3), Eq. (32) involves a dependence of Nu_w , in this case, on heat transfer length (Z).

Larachi et al. (2003) presented a correlation based on ANN to predict h_w . Inputs, outputs, and connectivity weights to estimate the wall heat transfer coefficient can be found in Table 9 of the above-mentioned article. It is essential to consult an erratum at the web site <http://www.gch.ulaval.ca/bgrandjean/tbr-pbc/tbr-pbc.html>.

The same general comments about this procedure are made when analyzing k_{er} (see Section 4.1.1) apply for h_w .

4.2.2 Analysis of the available experimental information and correlations for the wall heat transfer coefficient

The amount of experimental information about h_w is much lower than for k_{er} . One of the reasons relies on the fact that one of the experimental techniques (an adiabatic TBR, see Section 3.2) allows calculating k_{er} , but not h_w . At the same time, other authors did not report values of h_w (Borremans et al. 2003, Babu et al. 2007).

Regarding correlations specifically developed for HIR, a markedly different dependence of h_w on L arises. If such dependence is expressed as $h_w \propto L^n$, Eq. (29) corresponds to $n=0$, while in Eqs. (26b) and (30), values $n < 0.8$ and $n > 1$ arise, respectively. Summing up, it appears as risky to recommend a correlation for HIR.

A relatively higher number of correlations to predict h_w are available for LIR. The following discussion concerns specifically beds of spherical particles fed by air/water streams, due to the fact that most of the experimental data were obtained under these conditions.

Figure 9 shows a comparison of correlations to predict Nu_w vs. Re_L in LIR. Instead, the effect of Re_G is illustrated in Figure 10. A number of aspects are worth to be remarked. First, Figures 9 and 10 reveal a noticeable disagreement among correlations. Despite the fact that Nu_w increases as Re_L is increased for all correlations (Figure 9), the magnitude of the effect is quite different. From Figure 10, it can be concluded that the effect of Re_G can be regarded as negligible, except for the Larachi et al. (2003) correlation. In addition, the Matsuura et al. (1979b) and Pinto Moreira (2004) expressions lead to significantly low estimates of Nu_w under all the conditions analyzed.

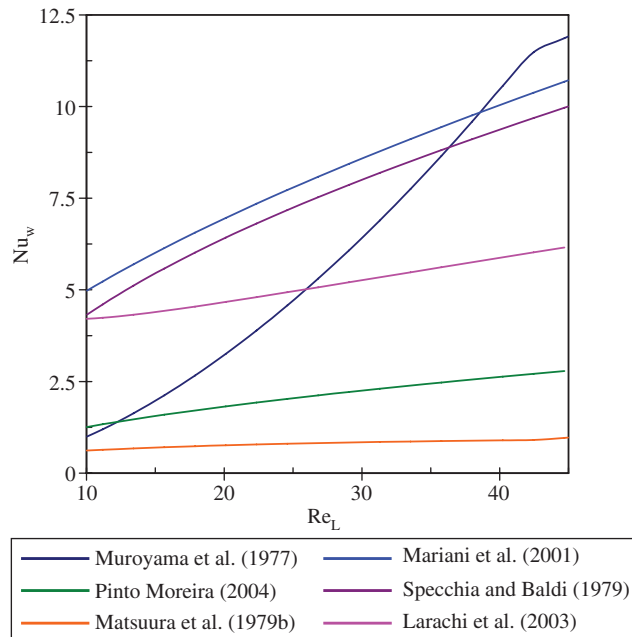


Figure 9: Nu_w vs. Re_L (air and water; $Re_g=4.3$, spherical particles, $d_p=0.003$ m, $d_t=0.00514$).

Regarding the effect of d_p , correlation (26a) is the only one that predicts an increase in h_w with d_p ($h_w \propto d_p^{0.7}$). The correlations of Matsuura et al. (1979b) and Larachi et al. (2003) do not show a clearly defined behavior due to the

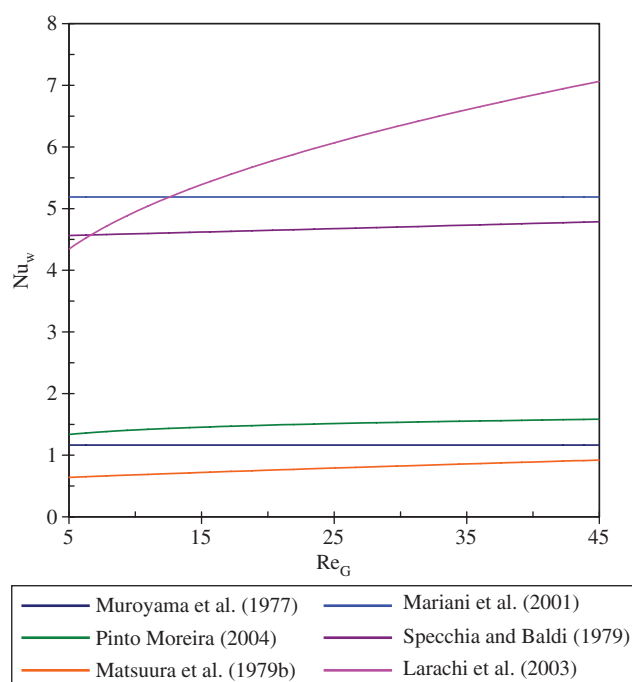


Figure 10: Nu_w vs. Re_G (air and water; $Re_L=10.9$; spherical particles, $d_p=0.003$ m, $d_t=0.00514$).

strong dependence on the remaining operating conditions. Eqs. (31) and (32) predict decreasing trends of h_w with d_p , although the magnitude of the effect varies significantly from one to another.

Tentatively, the correlation of Mariani et al. (2001) [when accounting for the specific restrictions given along with Eq. (31a)] may be employed for spherical particles and air-water flow in LIR. The correlations of Muroyama et al. (1977) and Larachi et al. (2003) cannot be recommended due to the unexpectedly large effect predicted for L and G, respectively, while the expressions of Matsuura et al. (1979b) and Pinto Moreira et al. (2004) provide very low estimates.

The effect of a has not been taken into account, except that Mariani et al. (2001) restrain their expression (31a) to values $a > 15$.

A set of 142 experimental data of h_w from different literature sources for air/water system and spherical particles in LIR shows a noticeable large scatter. Therefore, a comparison of the different correlations with experimental results is almost a nonviable task.

The availability of experimental information and correlations on h_w for particle shapes other than spheres and different fluids is strongly restricted. Therefore, the effects of these variables cannot be inferred with a proper degree of confidence.

It is a general conclusion that more systematic experimental studies are needed to develop a reliable correlation for estimating the wall heat transfer coefficient h_w .

4.3 Alternative models: two-zone model

It was previously noted that the effect of h_w on the radial heat exchange gains in significance as a decreases. With this effect in mind, Mariani et al. (2003) carried out experiments in beds of spheres at low (8.2 and 4.7) and large (17.2 and 34.3) aspect ratios. Mainly, the extracted values of h_w and, up to certain degree, also those of k_{er} at the low values of a (8.2 and 4.7) departed significantly from the trends showed at the larger values (17.2 and 34.3).

Mariani et al. (2003) postulated that the observed behaviors of h_w and k_{er} at low values of a are due to a failure of the 2DPPF model at these conditions. Thus, the authors noted that the 2DPPF model's assumption of uniform liquid distribution cannot be adequate at low values of a , as the presence of a highly ordered particle layer against the wall caused a high value of voidage in the zone (wall zone) from the wall up to a about a particle radius (see, e.g., Mariani et al. 2009), and consequently, larger liquid velocities than in the bed core arise in that zone (these

concepts were already pointed out in Section 4.2.1). As a result, about 50% of the liquid can flow in the wall zone when $a=5$. Besides, Mariani et al. (2003) split the overall thermal resistance close to the wall into an actual film resistance ($1/h_{w,w}$) just at the wall and a second resistance ($1/h_i$) at one particle radius from the wall, which stems in the restrained liquid lateralization closely around that distance. Outside the wall zone, the thermal behavior was modeled as in the 2DPPF model, in terms of the effective radial conductivity k_{er} . Altogether, these ideas give rise to formulate a two-zone (TZ) model to represent radial heat transfer in TBR (a sketch of the model is given in Figure 11).

The experimental data were reanalyzed according to the TZ model by adjusting h_i and k_{er} . A satisfactory interpretation of the experimental results was reached, with model parameters following continuous trends with operating conditions for the whole tested range of a .

Despite the TZ model providing a good prospect, additional experimental studies are necessary to identify with due certainty the model parameters at conditions different from those in Mariani et al. (2003). It is worth noting that this approach has also been followed for radial heat transfer in single-phase flow in packed beds (Asensio et al. 2014).

5 Heat transfer in packed beds with cocurrent up-flow

Taking into account that one of the most common alternatives to TBR is the use of packed bed reactors with

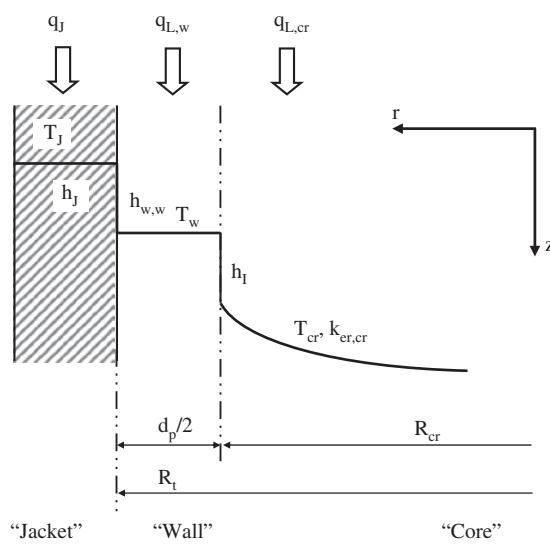


Figure 11: Sketch of the TZ model (Mariani et al. 2003).

cocurrent up-flow, it is interesting to summarize the available heat transfer studies in the latter system. A much lower number of articles about heat transfer in up-flow mode than in TBR can be found in the literature. Larachi et al. (2003) and Nili (2013) carried out a brief review on the subject, which reveals that, as for TBR, most of the experimental studies were performed using air and water flowing in beds of spherical particles. Also, the lack of experiments covering different flow regimes in the up-flow mode should be pointed out. This fact makes uncertain the assessment of the different correlations for radial effective thermal conductivity in the up-flow mode. In addition, for the wall heat transfer coefficient, Larachi et al. (2003) only mentioned the Sokolov and Yablokova correlation (1983). Later on, Pinto Moreira (2004) presented an expression to fit his experimental data.

The possibility of a direct comparison of heat transfer rates between the up-flow mode and TBR from data obtained by the same authors in the same set-up and using the same regression procedure is strongly restricted. Only some scarce results for the same conditions (gas and liquid flow rates and particle size) obtained by Colli Serrano (1993) and Pinto Moreira (2004) are available.

Summing up, it can be concluded that the experimental information about heat transfer in up-flow mode is much less complete than on TBR, and therefore, the comparison of heat transfer rates between the two systems requires further studies.

6 Conclusions and recommendations

A critical review of the available information about heat transfer between packed beds with gas-liquid cocurrent downflow and an external medium was undertaken.

The most widely used experimental set-up is a packed cylindrical tube heated (or cooled) through the tube wall.

Water and air at atmospheric pressure are the most extensively tested fluids. Experiments with organic liquids and under operative conditions typical of industrial processes (high temperatures and, particularly, high pressures) have not been systematically explored. Besides, most of the studies have been carried out employing spherical particles, and much scarcer data are available for cylindrical particles. To the best of our knowledge, no study on multilobe pellets, widely used in TBR, has been performed.

The 2DPPF model has been employed in almost all studies to interpret experimental results. From this model,

two thermal parameters arise: radial effective thermal conductivity, k_{er} , and wall heat transfer coefficient, h_w .

Literature correlations for k_{er} were analyzed and compared with a refined experimental database collected from the open literature. This database is restricted to results for spherical particles and air-water flow in LIR and HIR. It was checked that predictions of k_{er} from the Lamine et al. (1996) and Mariani et al. (2001) correlations show an acceptable good agreement with experimental data in LIR, while in HIR, only the Lamine et al. (1996) correlation gives reasonable estimates. Having available a wider database, new correlations for k_{er} , in LIR and HIR, were proposed. As expected, the performance of such correlations is better than those previously mentioned, when compared with the information from the database.

The amount of experimental data for h_w , as well as the number of correlations, is noticeably scarcer than for k_{er} . An analysis of the effect of operating and geometric conditions allows disclosing noticeable inconsistencies in some of the available correlations. Besides, important differences in values of h_w from such of correlations arise for comparable experimental conditions. A significant scatter of experimental results from different sources was also evident. In this context, the expression proposed by Mariani et al. (2001), Eq. (31a), can be tentatively employed for spherical particles and air-water flow in LIR. Nonetheless, it is a general conclusion that more systematic experimental studies are needed to develop a reliable correlation for estimating the wall heat transfer coefficient h_w .

The possibility of developing reliable tools to predict heat transfer rates in TBR calls for additional efforts in different directions. On the one hand, additional experimental studies covering different particle shapes and nonaqueous liquids are needed. On the other hand, the assumption of uniform liquid distribution in the bed cross-section and the use of a heat transfer coefficient h_w located just at the wall, as required by the standard 2DPPF model, have shown to be apparently inappropriate for low bed-to-particle diameter ratios (a). These features have been removed in the TZ model proposed by Mariani et al. (2003), and thus, a better interpretation of experimental results was achieved. The model introduces additional parameters (ratio of liquid velocities in the zones and a heat resistance between them), which, despite presenting a clear physical meaning, require further experimental efforts for their estimation covering the effect of practical ranges of geometrical and operating variables.

Nomenclature

a	bed aspect ratio, d_i/d_{eq} , dimensionless
c_p	specific heat, $J/(kg \cdot ^\circ C)$
d_p	nominal particle diameter, m
d_{eq}	equivalent diameter, m
d_t	tube diameter, m
G	superficial gas mass flow rate, $kg/(m^2 \cdot s)$
h_c	jacket heat transfer coefficient, $W/(m^2 \cdot ^\circ C)$
h_T	overall heat transfer coefficient in the bed, $W/(m^2 \cdot ^\circ C)$
k	fluid thermal conductivity, $W/(m \cdot ^\circ C)$
L	superficial liquid mass velocity, $kg/(m^2 \cdot s)$
N	number of experimental data points, dimensionless
Nu_w	Nusselt number, $h_w d_{eq}/k_L$, dimensionless
Pr	Prandtl number, $c_p \mu /k$, dimensionless
r	radial coordinate
Re	Reynolds number, $G d_{eq}/\mu$ or $L d_{eq}/\mu$, dimensionless
R_t	tube radius, m
S_p	external surface area of the particle, m ²
S	bed cross-section area, m ²
T	temperature, K
V_p	particle volume, m ³

Greek symbols

ε	global bed void fraction, -
ϕ	sphericity, -
μ	dynamic viscosity, Pa s
β_L	total liquid saturation, -

Subscripts

0	bed inlet
c	heating
E	bed exit
G	gas
L	liquid
r	radial
w	wall

Acknowledgments: The authors thank the following Argentine institutions for financial support: ANPCyT-SECyT (PICT 1641), CONICET (PIP 0304), and UNLP (PID 11/I177). N.J.M., O.M.M., and G.F.B. are research members of CONICET and M.J.T. holds a fellowship from CONICET.

References

Al-Dahhan MH, Larachi F, Dudukovic MP, Laurent A. High-pressure trickle-bed reactors: a review. *Ind Eng Chem Res* 1997; 36: 3292–3314.

- Ancheyta J. Modeling and simulation of catalytic reactors for petroleum refining. New Jersey: J. Wiley & Sons Inc. 2011.
- Asensio DA, Zambon MT, Mazza GD, Barreto GF. Heterogeneous two-region model for low-aspect ratio fixed-bed catalytic reactors. Analysis of fluid-convective contributions. *Ind Eng Chem Res* 2014; 53: 3587–3605.
- Babu BV, Rao VG. Thermal resistance models for effective heat transfer parameters in trickle bed reactors. *Proceedings of Sixth International Symposium on Catalysis in Multiphase Reactors (CAMURE-6) and fifth International Symposium on Multifunctional Reactors (ISM-R-5)*. NCL-Pune, January 14, 2007.
- Babu BV, Sastry KKN. Estimation of heat transfer parameters in a trickle-bed reactor using differential evolution and orthogonal collocation. *Comp Chem Eng* 1999; 23: 327–339.
- Babu BV, Shah KJ, Rao VG. Lateral mixing in trickle bed reactors. *Chem Eng Sci* 2007; 62: 7053–7059.
- Bandari MR, Behjat Y, Shahhosseini S. CFD investigation of hydrodynamic and heat transfer phenomena around trilobe particles in hydrocracking reactor. *Int J Chem React Eng* 2012; 10.
- Bauer R, Schlünder EU. Effective radial thermal conductivity of packings in gas flow. Part II: thermal conductivity of the packing fraction without gas flow. *Int Chem Eng* 1978a; 18: 189–204.
- Bauer R, Schlünder EU. Effective radial thermal conductivity of packings in gas flow. Part I: convective transport coefficient. *Int Chem Eng* 1978b; 18: 181–188.
- Boelhouwer JG, Piepers HW, Drinkenburg AAH. Particle-liquid heat transfer in trickle-bed reactors. *Chem Eng Sci* 2001; 56: 1181–1187.
- Borkink JGH, Westerterp KR. Determination of effective heat transport coefficients for wall-cooled packed bed. *Chem Eng Sci* 1992; 47: 2337–2342.
- Borremans D, Rode S, Carré P, Wild G. The influence of the periodic operation on the effective radial thermal conductivity in trickle bed reactors. *Can J Chem Eng* 2003; 81: 795–801.
- Bressa SP, Ardiaca NO, Martínez OM, Barreto GF. Analysis of operating variables in the catalytic purification of 1-butane in a trickle-bed. *Chin J Chem Eng* 1998; 6: 103–115.
- Chu CF, Ng KM. Effective thermal conductivity in trickle-bed reactors: application of effective medium theory and random walk analysis. *Chem Eng Commun* 1985; 37: 127–140.
- Colli Serrano MT. Hydrodynamique et transfert de chaleur dans un reacteur fil fixe gaz-liquide-solide. PhD dissertation in French: Institut National Polytechnique de Lorraine, 1993.
- Crine M. Heat transfer phenomena in trickle-bed reactors. *Chem Eng Commun* 1982; 19: 99–114.
- Dixon A. Thermal resistance models of packed-bed effective heat transfer parameters. *AIChE J* 1985; 31: 826–834.
- Dixon AG. Fixed bed catalytic reactor modeling – the radial heat transfer problem. *Can J Chem Eng* 2012; 90: 505–527.
- Dudukovic MP, Larachi F, Mills PL. Multiphase reactors – revisited. *Chem Eng Sci* 1999; 54: 1975–1995.
- Gianetto A, Specchia V. Trickle-bed reactors: state of art and perspectives. *Chem Eng Sci* 1992; 47: 3197–3213.
- Grosser K, Carbonell RG, Cavero A, Sáez AE. Lateral thermal dispersion in gas-liquid cocurrent downflow through packed beds. *AIChE J* 1996; 42: 2977–2983.
- Hashimoto K, Murayama K, Nagata S, Fujiyoshi K. Effective radial thermal conductivity in concurrent flow of gas and liquid

- through packed bed. *Kagaku Kogaku Ronbunshu* 1976; 2: 53–59.
- Heidari A, Hashemabadi SH. Numerical evaluation of the gas-liquid interfacial heat transfer in the trickle flow regime of packed beds at the micro and meso-scale. *Chem Eng Sci* 2013; 104: 674–689.
- Jess A, Kern C. Influence of particle size and single-tube diameter on thermal behavior of Fischer-Tropsch reactors. *Chem Eng Technol* 2012; 35: 379–386.
- Joubert R, Nicol W. Multiplicity behavior of trickle flow liquid-solid mass transfer. *Ind Eng Chem Res* 2009; 48: 8387–8392.
- Krishna R, Sie ST. Fundamentals and selection of advanced Fischer-Tropsch reactors. *Appl Catal A* 1999; 186: 55–70.
- Lamine AS, Gerth L, Le Gall H, Wild G. Heat transfer in a packed bed reactor with cocurrent downflow of a gas and a liquid. *Chem Eng Sci* 1996; 51: 3813–3827.
- Larachi F, Belfares L, Iliuta I, Grandjean BPA. Heat and mass transfer in cocurrent gas-liquid packed beds. Analysis, recommendations, and new correlations. *Ind Eng Chem Res* 2003; 42: 222–242.
- Larachi F, Laurent A, Midoux N, Wild G. Experimental study of a trickle-bed reactor operating at high pressure drop and liquid saturation. *Chem Eng Sci* 1991; 46: 1233–1246.
- Larachi F, Laurent A, Wild G, Midoux N. Effet de la pression sur la transition ruisseau-pulsé dans le réacteurs catalytiques à lit fixe arrosé. *Can J Chem Eng* 1993; 71: 319–321.
- Lemcoff NO, Pereira Duarte SI, Martínez OM. Heat transfer in packed beds. *Rev Chem Eng* 1990; 6: 229–292.
- Levec J, Pintar A. Catalytic oxidation of aqueous solutions of organics. An effective method for removal of toxic pollutants from waste waters. *Catal Today* 1995; 24: 51–58.
- Loudon D, van der Merwe W, Nicol W. Multiple hydrodynamic states in trickle flow: quantifying the extent of pressure drop, liquid holdup and gas-liquid mass transfer variation. *Chem Eng Sci* 2006; 61: 7551–7562.
- Marcandelli C, Wild G, Lamine AS, Bernard JR. Measurement of local particle-fluid heat transfer coefficient in trickle-bed reactors. *Chem Eng Sci* 1999; 54: 4997–5002.
- Mariani NJ. Transferencia de calor en sistemas multifásicos. PhD Dissertation in Spanish: Universidad Nacional de La Plata, 2000.
- Mariani NJ, Martínez OM, Barreto GF. Evaluation of heat transfer parameters in packed beds with cocurrent downflow of liquid and gas. *Chem Eng Sci* 2001; 56: 5995–6001.
- Mariani NJ, Martínez OM, Barreto GF. Experimental evaluation of the wall effect on liquid distribution in trickle beds. Proceedings of ENPROMER 2005, Paper No 0173, 4th Mercosur Congress on Process Systems Engineering and 2nd Mercosur Congress on Chemical Engineering, Rio das Pedras: Rio de Janeiro, Brazil, 2005.
- Mariani NJ, Mazza GD, Martínez OM, Barreto GF. The distribution of particles in cylindrical packed beds. *Trends Heat Mass Momentum Transfer* 1998; 4: 95–114.
- Mariani NJ, Mazza GD, Martínez OM, Cukierman AL, Barreto GF. On the influence of liquid distribution on heat transfer parameters in trickle bed systems. *Can J Chem Eng* 2003; 81: 814–820.
- Mariani NJ, Salvat WI, Campesi MA, Barreto GF, Martínez OM. Evaluation of structural properties of cylindrical packed beds using numerical simulations and tomographic experiments. *Int J Chem React Eng* 2009; 7: 1–18.
- Martínez OM, Casanello MC, Cukierman AL. Three-phase fixed bed catalytic reactors: application to hydrotreatment processes. *Trends Chem Eng* 1994; 2: 393–453.
- Mary G, Chaouki J, Luck F. Trickle-bed laboratory reactors for kinetic studies. *Int J Chem React Eng* 2009; 7: 1–70.
- Matsuura A, Hitaka Y, Akehata T, Shirai T. Effective radial thermal conductivity in packed beds with gas-liquid downflow. *Kagaku Kogaku Ronbunshu* 1979a; 5: 269–274.
- Matsuura A, Hitaka Y, Akehata T, Shirai T. Apparent wall heat transfer coefficient in packed beds with downward concurrent gas-liquid flow. *Kagaku Kogaku Ronbunshu* 1979b; 5: 263–268.
- Mederos FS, Ancheyta J, Chen J. Review on criteria to ensure ideal behaviors in trickle-bed reactors. *Appl Catal A* 2009; 355: 1–19.
- Mousazadeh F. Hot spot formation in trickle bed reactors. PhD Dissertation: Delft University of Technology, 2013.
- Mousazadeh F, van den Akker HHA, Mudde RF. Eulerian simulation of heat transfer in a trickle bed reactor with constant wall temperature. *Chem Eng J* 2012; 207–208: 675–682.
- Muroyama K, Hashimoto K, Tomita T. Heat transfer from the wall in gas-liquid concurrent packed beds. *Kagaku Kogaku Ronbunshu* 1977; 3: 612–616.
- Nili S. Investigation of thermal conductivity of iron-silica magnetically stabilized porous structure. Master of Science Dissertation: University of Florida, 2013.
- Pinto Moreira MF. Avaliação de aspectos fluidodinâmicos e da transferência de calor em leito fixo com escoamento gás-líquido concorrente vertical. PhD Dissertation in Portuguese: Universidade Federal de São Carlos, 2004.
- Pinto Moreira MF, Ferreira MC, Teixeira Freire J. Evaluation of pseudohomogeneous models for heat transfer in packed beds with gas flow and gas-liquid cocurrent downflow and upflow. *Chem Eng Sci* 2006; 61: 2056–2068.
- Ranade VV, Chaudhari RV, Gunjal PR. Trickle bed reactors: reactor engineering & applications, Oxford, UK: Elsevier B.V., 2011.
- Ranz WE. Friction and transfer coefficients for single particles and packed beds. *Chem Eng Prog* 1952; 48: 247–253.
- Saroha AK, Nigam KDP. Trickle bed reactors. *Rev Chem Eng* 1996; 12: 207–347.
- Sokolov VN, Yablokova M. Thermal conductivity of a stationary granular bed with upward gas-liquid flow. *J Appl Chem USSR (Zh. Prikl. Khim.)* 1983; 56: 551–553.
- Specchia V, Baldi G. Heat transfer in trickle-bed reactors. *Chem Eng Commun* 1979; 3: 483–499.
- Weekman V Jr, Myers J. Fluid-flow characteristics of concurrent gas-liquid flow in packed beds. *AIChE J* 1964; 10: 951–957.
- Weekman V Jr, Myers J. Heat characteristics of concurrent gas-liquid flow in packed beds. *AIChE J* 1965; 11: 13–17.
- Wijffels JB, Verloop J, Zuiderweg FJ. Wetting of catalyst particles under trickle flow conditions. *ACS Monograph Ser* 1974; 133: 151–163.
- Yagi S, Kunii D. Studies on effective thermal conductivities in packed bed. *AIChE J* 1957; 3: 373–381.
- Zhu X. A study of radial heat transfer in fixed bed Fischer-Tropsch synthesis reactors. PhD Dissertation: University of the Witwatersrand, 2013.
- Zhukova TB, Pisarenko VN, Kafarov VV. Modeling and design of industrial reactors with a stationary bed of catalyst and two-phase gas-liquid flow. A review. *Int Chem Eng* 1990; 30: 57–102.
- Zou RP, Yu AB. Packing of spheres in a cylindrical container: the thickness effect. *Chem Eng Sci* 1995; 50: 1504–1150.

Bionotes



María J. Taulamet

PROIRQ, Facultad de Ingeniería,
Departamento de Ingeniería Química,
UNLP, La Plata, Argentina; and Centro de
Investigación y Desarrollo en Ciencias
Aplicadas “Dr. J. J. Ronco” (CINDECA), CCT
La Plata-CONICET-UNLP, calle 47 No. 257, CP
B1900AJK, La Plata, Argentina

María J. Taulamet is an Assistant Professor of Chemical Engineering at the Engineering Faculty of the Universidad Nacional de La Plata (UNLP), La Plata, Argentina. She holds a fellowship from CONICET (Consejo Nacional de Investigaciones Científicas y Técnicas, Argentina) at CINDECA (Centro de Investigación y Desarrollo en Ciencias Aplicada “Dr. Jorge J. Ronco”) to develop her PhD program at UNLP. She received a BSc degree (“Ingeniero Químico”) from the UNLP. Her research areas include heat and mass transfer, catalytic kinetics, and modeling and simulation of chemical reactors.



Néstor J. Mariani

PROIRQ, Facultad de Ingeniería,
Departamento de Ingeniería Química,
UNLP, La Plata, Argentina; and Centro de
Investigación y Desarrollo en Ciencias
Aplicadas “Dr. J. J. Ronco” (CINDECA), CCT
La Plata-CONICET-UNLP, calle 47 No. 257, CP
B1900AJK, La Plata, Argentina

Néstor J. Mariani is a full Professor of Mechanical Engineering at the Engineering Faculty of the Universidad Nacional de La Plata (UNLP), La Plata, Argentina. He is also a research member of CONICET (Consejo Nacional de Investigaciones Científicas y Técnicas, Argentina) at CINDECA (Centro de Investigación y Desarrollo en Ciencias Aplicada “Dr. Jorge J. Ronco”). He received a BSc degree (“Ingeniero Químico”) and a PhD diploma from the UNLP. His major research areas include heat and mass transfer and modeling and simulation of chemical reactors. Professor Mariani has published more than 30 articles in peer-reviewed journals and he has also participated in numerous conferences and technical reports to industrial companies.



Guillermo F. Barreto

PROIROQ, Facultad de Ingeniería,
Departamento de Ingeniería Química,
UNLP, La Plata, Argentina; and Centro de
Investigación y Desarrollo en Ciencias
Aplicadas “Dr. J. J. Ronco” (CINDECA), CCT
La Plata-CONICET-UNLP, calle 47 No. 257, CP
B1900AJK, La Plata, Argentina

Guillermo F. Barreto is a full Professor of Chemical Engineering at the Engineering Faculty of the Universidad Nacional de La Plata (UNLP), La Plata, Argentina. He is also a research member of CONICET (Consejo Nacional de Investigaciones Científicas y Técnicas, Argentina) at CINDECA (Centro de Investigación y Desarrollo en Ciencias Aplicada “Dr. Jorge J. Ronco”). He received a BSc degree (“Ingeniero Químico”) from the UNLP and his PhD from the University of London, UK, in 1984. His research interests include modeling and simulation of chemical reactors, catalytic kinetics, and heat and mass transfer. Professor Barreto has more than 90 publications in refereed journals, numerous contributions in conferences, and technical reports to industrial companies.



Osvaldo M. Martínez

PROIROQ, Departamento de Ingeniería
Química, Facultad de Ingeniería, UNLP, La
Plata, Argentina,
ommartin@ing.unlp.edu.ar;
and Centro de Investigación y Desarrollo
en Ciencias Aplicadas “Dr. J. J. Ronco”
(CINDECA), CCT La Plata-CONICET-UNLP, calle
47 No. 257, CP B1900AJK, La Plata, Argentina

Osvaldo M. Martínez received a BSc degree in Chemical Engineering from the National University of La Plata, Argentina, in 1977. He obtained the Diplome de Recherche Universitaire (DRU) from Institut National Polytechnique de Toulouse, France, in 1989. His major interests are heat transfer in packed beds, analysis and simulation of trickle bed reactors, modeling of packed-bed reactors, removal of volatile organic compounds (VOCs) from air streams, and selective hydrogenation. At present, he is a researcher of CONICET (Argentina) and a full professor in the Chemical Engineering Department at the National University of La Plata.